not Ser-5–phosphorylated Pol II could be detected at the downstream region after day 5.5, which is consistent in part with the recent finding that Pol II-S5P is localized to promoters, whereas Pol II-S2P can be observed in coding regions (*25*). The finding that both Ser-5– and Ser-2–phosphorylated forms of Pol II were present at the α_1-AT promoter from the day of recruitment and long before transcription could be detected suggests that CTD phosphorylation is not sufficient for Pol II release. This could occur only when NUC-2 became remodeled, pointing to a previously unknown regulatory function of nucleosome structure. When situated around the transcription start site, the nucleosome may act as a barrier that controls the escape of RNA pol II from the promoter. In the case of the α_1-AT gene, nucleosome reconfiguration is the final determining step of the initiation process.

References and Notes

1. B. Lemon, R. Tjian, *Genes Dev.* **14**, 2551 (2000).
2. K. Struhl, *Cell* **98**, 1 (1999).
3. C. J. Fry, C. L. Peterson, *Curr. Biol.* **11**, R185 (2001).
4. C. L. Peterson, J. L. Workman, *Curr. Opin. Genet. Dev.* **10**, 187 (2000).
5. R. E. Kingston, G. J. Narlikar, *Genes Dev.* **13**, 2339 (1999).
6. B. D. Strahl, C. D. Allis, *Nature* **403**, 41 (2000).
7. M. P. Cosma, T. Tanaka, K. Nasmyth, *Cell* **97**, 299 (1999).
8. M. P. Cosma, S. Panizza, K. Nasmyth, *Mol. Cell* **7**, 1213 (2001).
9. L. T. Bhoite, Y. Yu, D. J. Stillman, *Genes Dev.* **15**, 2457 (2001).
10. T. Agalioti *et al.*, *Cell* **103**, 667 (2000).
11. M. D. Peterson, M. S. Mooseker, *J. Cell Sci.* **102**, 581 (1992).
12. D. H. Perlmutter *et al.*, *J. Biol. Chem.* **264**, 9485 (1989).
13. P. Monaci, A. Nicosia, R. Cortese, *EMBO J.* **7**, 2075 (1988).
14. C. Hu, D. H. Perlmutter, *Am. J. Physiol.* **276**, G1181 (1999).
15. K. Struhl, *Genes Dev.* **12**, 599 (1998).
16. Supplementary information can be found on *Science* Online at www.sciencemag.org/cgi/content/full/295/5561/1901/DC1.
17. B. Bell, L. Tora, *Exp. Cell Res.* **246**, 11 (1999).
18. S. R. Albright, R. Tjian, *Gene* **242**, 1 (2000).
19. F. J. Dilworth, C. Fromental-Ramain, K. Yamamoto, P. Chambon, *Mol. Cell* **6**, 1049 (2000).
20. E. Soutoglou *et al.*, *EMBO J.* **20**, 1984 (2001).
21. A. H. Hassan, K. E. Neely, J. L. Workman, *Cell* **104**, 817 (2001).
22. P. Syntichaki, I. Topalidou, G. Thireos, *Nature* **404**, 414 (2000).
23. E. Soutoglou, N. Katrakili, I. Talianidis, *Mol. Cell* **5**, 745 (2000).
24. M. E. Dahmus, *J. Biol. Chem.* **271**, 19009 (1996).
25. P. Komarnitsky, E.-J. Cho, S. Buratowsky, *Genes Dev.* **14**, 2452 (2000).
26. M. E. Greenberg, in *Current Protocols in Molecular Biology*, M. Ausubel *et al.*, Eds. (Wiley, New York, 1999) vol. 1, chap. 4.
27. C. E. McPherson, E. Y. Shim, D. S. Friedman, K. S. Zaret, *Cell* **75**, 387 (1993).

28. Supported by grants from the Greek General Secretariat for Science and Technology (PENED-99ED-636), European Union (HPRN-CT-2000-00087), and Human Frontier Science Program (RGP-0024). We thank L. Tora and Y. Nakatani for antibody reagents, N. Katrakili for expert technical assistance, and P. Hatzis and G. Thireos for helpful discussions and comments on the manuscript.

26 November 2001; accepted 18 January 2002

Purkinje cell degeneration (*pcd*) Phenotypes Caused by Mutations in the Axotomy-Induced Gene, *Nna1*

Angeles Fernandez-Gonzalez,[1]* Albert R. La Spada,[2]* Jason Treadaway,[1] Jason C. Higdon,[1] Belinda S. Harris,[3] Richard L. Sidman,[4] James I. Morgan,[1] Jian Zuo[1]†

The classical recessive mouse mutant, *Purkinje cell degeneration* (*pcd*), exhibits adult-onset degeneration of cerebellar Purkinje neurons, retinal photoreceptors, olfactory bulb mitral neurons, and selected thalamic neurons, and has defective spermatogenesis. Here we identify *Nna1* as the gene mutated in the original *pcd* and two additional *pcd* alleles (*pcd*^{2J} and *pcd*^{3J}). *Nna1* encodes a putative nuclear protein containing a zinc carboxypeptidase domain initially identified by its induction in spinal motor neurons during axonal regeneration. The present study suggests an unexpected molecular link between neuronal degeneration and regeneration, and its results have potential implications for neurodegenerative diseases and male infertility.

Strains of mice harboring mutations that affect the nervous system have provided important insights into normal and aberrant neural development and function (*1–3*). Although the genes responsible for many of the classical neurological mutants have been identified, the *Purkinje cell degeneration* (*pcd*) gene remains elusive. Unlike many mouse mutants in which neuronal loss occurs during development (*2*, *3*), *pcd* is unusual in that neurodegeneration occurs after weaning, when most synaptic circuitries are established. Thus, the identification of the gene responsible for the *pcd* phenotype could provide a key molecular entry point into pathways or processes underlying other neurodegenerative disorders in humans.

The original *pcd* mutation (referred to here as "*pcd*^{1J}", to distinguish it from later-occurring *pcd* mutations) arose spontaneously in the C57BR/cdJ strain and exhibits ataxia resulting from loss of cerebellar Purkinje cells during early adulthood (*4*, *5*). Populations of thalamic neurons also degenerate between postnatal days 50 and 60 in *pcd*^{1J} (*6*, *7*), whereas degeneration of retinal photoreceptors and olfactory bulb mitral cells progresses slowly over a year (*8–11*). Also, adult male *pcd*^{1J} mice are infertile because they have reduced numbers of sperm that are abnormally shaped and nonmotile (*5*, *12*). Two additional *pcd* alleles, *pcd*^{2J} and *pcd*^{3J}, arose spontaneously in SM/J and BALB/cByJ mouse strains, respectively. The *pcd*^{2J} allele was maintained in C57BL/6J congenic lines for >15 backcross generations. The phenotypes of *pcd*^{1J} and *pcd*^{3J} homozygotes were nearly iden-

[1]Department of Developmental Neurobiology, St. Jude Children's Research Hospital, Memphis, TN 38105, USA. [2]Department of Laboratory Medicine and Division of Medical Genetics (Medicine), University of Washington, Seattle, WA 98195–7110, USA. [3]The Jackson Laboratory, Bar Harbor, ME 04609, USA. [4]Harvard Medical School and Department of Neurology, Beth Israel Deaconess Medical Center, Boston, MA 02115, USA.

*These authors contributed equally to this work.
†To whom correspondence should be addressed. E-mail: jian.zuo@stjude.org

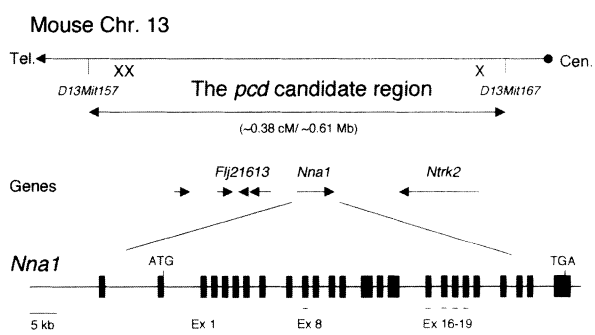

Fig. 1. Genetic mapping of *pcd* and gene structure of *Nna1*. The *pcd* locus was mapped to mouse chromosome 13 between *D13Mit167* and *D13Mit157*. Three crossovers (two telomeric, "XX" and one centromeric, "X") defined the boundaries of the *pcd* candidate region. The *pcd* cosyntenic region of human (9q21.33–9q22.1) contains six predicted genes (indicated by lines and their 3′ ends indicated by arrows); *Ntrk2* and *Flj21613* flank *Nna1*. Filled squares, exons; ATG, initiation codon; TGA, stop codon. Exons 8 and 16 to 19 (underlined) were used as probes for Northern and in situ hybridization analyses.

tical, and allelic tests between them were positive (data not shown). However, the *pcd*^{2J} mutants develop ataxia later than *pcd*^{1J} mice and are more mildly affected. Thalamic neurons do not degenerate in *pcd*^{2J} homozygotes on the original SM/J or the congenic C57BL/6J backgrounds, even at one year of age (data not shown). Also, many *pcd*^{2J} homozygous males are fertile.

To refine the position of *pcd* on mouse chromosome 13, we used a previously reported CAST/Ei × *pcd*^{1J} cross (*13*) and set up additional crosses (CAST/Ei × *pcd*^{1J}, MOLG/Dn × *pcd*^{1J}, and CAST/Ei × *pcd*^{3J}). We analyzed a total of 419 offspring (838 meiotic recombination events), 198 in the CAST/Ei times *pcd*^{1J} cross, 86 in the MOLG/Dn times *pcd*^{1J} cross, and 135 in the CAST/Ei times *pcd*^{1J} cross, with polymorphic DNA markers (*14*). Two critical crossovers defined the telomeric boundary at *D13Mit157*, and a third marked the centromeric boundary at *D13Mit167* (Fig. 1). Thus, the *pcd* candidate region was refined to a genomic segment of 0.61 ± 0.33 megabases.

Using a mouse genomic sequence database (Celera Discovery System v. 3.01), we found the *pcd* candidate region to be cosyntenic with a region on human 9q21.33–9q22.1, which contains six identified or predicted genes. A previously identified gene, *Nna1* [*NNA1* or *KIAA1035* in humans (*15*)], spans >100 kb in the mouse *pcd* region (Fig. 1). *Nna1* was first identified in a screen for inducible genes in a sciatic nerve transection paradigm, and it is expressed in developing and adult brain, spinal motor neurons undergoing axon regeneration, testis, and heart (*15*). Nna1 is a putative nuclear protein that contains a zinc carboxypeptidase domain and is structurally most related to the adipocyte enhancer binding protein 1 (AEBP1) (*15*).

To determine if *Nna1* is altered in *pcd* mice, we performed Northern analyses (*16*) on RNA isolated from cerebellum, cerebral cortex, testis, and heart of wild-type and homozygous adult *pcd*^{1J}, *pcd*^{2J}, and *pcd*^{3J} animals. In all three *pcd* alleles, *Nna1* messenger RNA (mRNA) was either dramatically reduced or altered in structure (data not shown) (Fig. 2), whereas mRNAs of two genes immediately flanking *Nna1* were unchanged (Web fig.1, available on *Science* Online at www.sciencemag.org/cgi/content/full/295/5561/1904/DC1).

In *pcd*^{3J}, *Nna1* mRNA in brain and testis was reduced in abundance and size when a probe derived from exons 16 to 19 was used (Fig. 2). However, the *Nna1* mRNA was undetectable when an exon 8 probe was used. The absence of exon 8 in *pcd*^{3J} brain and testis was confirmed with the use of in situ hybridization. Reverse transcriptase–polymerase chain reaction (RT-PCR) analysis established that a splice junction was formed between exons 5 and 9, thereby introducing a stop codon that truncates Nna1 (Fig. 3, A and B). Genomic analysis of *pcd*^{3J} revealed a deletion of ~12.2-kb between intron 5 and exon 8 that causes the aberrant mRNA (Fig. 3, C and D).

In *pcd*^{2J}, *Nna1* mRNA was undetectable using the exon 16 to 19 probe in cerebellum, brain, and heart but was present at reduced levels in testis (data not shown) (Fig. 2). All exons of *Nna1* are intact in *pcd*^{2J}. However, we identified an ~7.8-kb insertion in intron 13 of the *Nna1* gene (Fig. 4A). This 7.8 kb insertion (GenBank accession number AF457126) appears to be a long-period interspersed sequence nor a intracisternal A particle (LINE and IAP, respectively), but rather contains repetitive sequences nearly identical to an ~ 7.8 kb segment of Mus musculus α/δ T cell receptor locus on chromosome 14 (GenBank accession number AE008685). Intragenic suppression by transposable elements is well known and underlies another classic cerebellar mouse mutant, *vibrator* [(*17*), and references therein].

In *pcd*^{1J}, the *Nna1* mRNA was undetectable in all tissues examined except for testis where it was reduced approximately 20-fold, substantially more than in *pcd*^{2J} (data not shown) (Fig. 2). Presumably, the level of *Nna1* in *pcd*^{2J} testis is sufficient to support spermatogenesis, whereas the level is inadequate in *pcd*^{1J}. As the sequence of the *Nna1* mRNA is identical to that of wild-type and there are no overt exonic mutations (data not shown), we expect that the *pcd*^{1J} mutation is in a regulatory region of *Nna1*. We propose, in accordance with standard rules (*18*), that the *pcd* mutations hereafter be assigned the following gene symbols: *Nna1*$^{pcd\text{-}1J}$, *Nna1*$^{pcd\text{-}2J}$, and *Nna1*$^{pcd\text{-}3J}$.

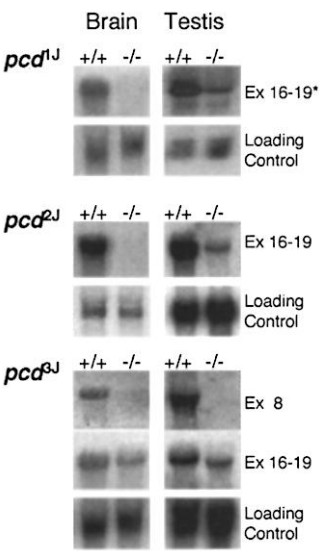

Fig. 2. Northern blot analysis of *Nna1* in brain and testis of *pcd*^{1J}, *pcd*^{2J}, and *pcd*^{3J} mice. Total RNA from brain and testis of adult mutant (−/−) and wild-type (+/+) littermates were analyzed by Northern blotting with the sequential use of *Nna1*-specific and loading control probes. *Nna1* probes for exon 8 (nucleotide 798–1007 of GenBank accession number NM_023328) and exons 16 to 19 (nucleotide 2408–2976 of NM_023328) were used. For *pcd*^{1J} testis (asterisk), a probe (nucleotide 2260–3106 of GenBank accession number NM_023328) was used. Loading control probes were from *Gapdh* (*pcd*^{1J} testis, nucleotide 143–363 of NM_008084) and *HO-2* (all other panels, nucleotide 872–1067 of GenBank accession number, J05405).

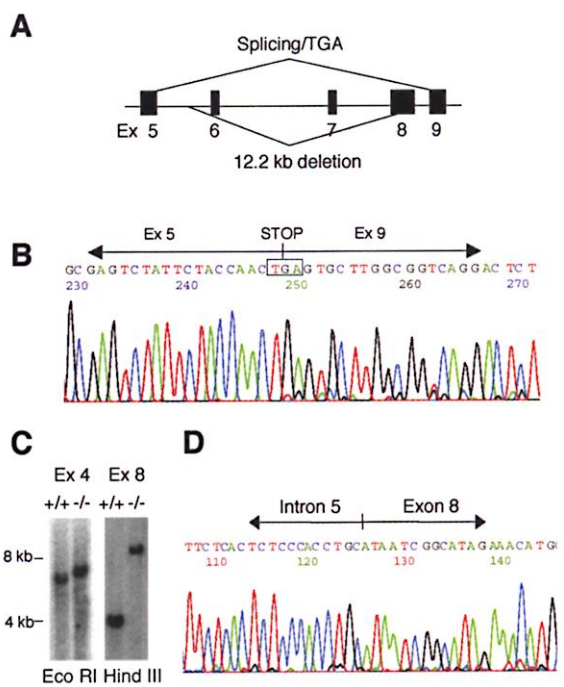

Fig. 3. Mutation in *pcd*^{3J}. (**A**) Diagram of genomic deletion and resulting alternative splicing. In *pcd*^{3J}−/−, a ~12.2-kb genomic deletion occurred between intron 5 and exon 8 (nucleotide 876 of NM_023328). This leads to alternative splicing between exon 5 (nucleotide 665 of NM_023328) and exon 9, thereby introducing a stop codon and yielding a truncated protein. (**B**) Forward sequence of a RT-PCR product from *pcd*^{3J}−/− brain. Primers used for RT-PCR and sequencing were from exon 4 (5′-GAGCGAGTTTCTTAGTTGCC-3′) and exon 11 (5′-CATCAACAAGCTCGGGGAAAAGG-3′). Box indicates splice junction between exons 5 and 9, forming a stop codon. (**C**) Genomic Southern blot analysis of *pcd*^{3J}. The exon 4 probe was amplified with the use of primers as follows: 5′-GTCCACTACGTGAAGATAGG-3′ and 5′-GTTACAAAGATGGCTCTAGGGTC-3′. The exon 8 probe was as in Fig. 2. (**D**) Forward sequence of a genomic PCR product of *pcd*^{3J}−/− showing deletion junction. Primers from intron 5 (5′-CTGTAGTGCAGGTCCTGCCTGC-3′) and exon 8 were used for PCR and sequencing.

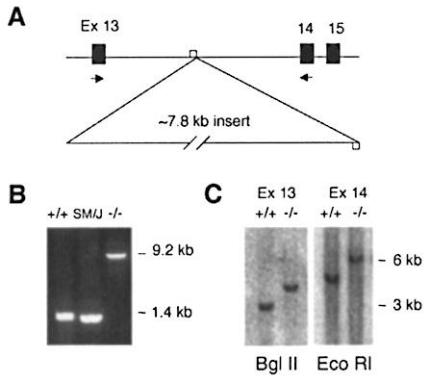

Fig. 4. Mutation in *pcd*^{2J}. (**A**) Diagram of the ~7.8-kb insertion within intron 13 in *pcd*^{2J}. Boxes indicate the duplicated target hexamers, CCTTAG (Fig. 4C), that result from the insertion. (**B**) Long-distance PCR analyses of intron 13 of *pcd*^{2J} (*22*). Arrows in (A) are the two primers used (Ex13F, 5′-CCAAGACATCGAGAGGCTGATAC-3′, and Ex14R, 5′-GAATTACTTTGCGCAGATTCC-3′). (**C**) Genomic Southern blot analyses of the *pcd*^{2J} mutation. Exon 13 and 14 probes were obtained with the use of primer pairs Ex13F and Int13R4 (5′-GAGAACAGCAACAATGAAGCG-3′) and Ex14R and Int13F4 (5′-GAGCCTTCCGTGGTAGCTAACG-3′), respectively.

Chimera studies in mice have shown that *pcd* behaves as a cell-autonomous allele (*19*). To determine if *Nna1* is expressed in the cell types affected in *pcd*, we performed in situ hybridization (*16*) on one-month-old wild-type mice. *Nna1* was expressed throughout the brain (Fig. 5, F, G, and H), retina (Fig. 5I),and testis (Fig. 5J) [see also (*15*)]. Notably, prominent expression of *Nna1* mRNA was detected in Purkinje cells of cerebellum (Fig. 5F, inset), mitral cells of the olfactory bulb (Fig. 5H), neurons in the thalamus (Fig. 5G), and photoreceptors of the retina (Fig. 5I), which all degenerate in *pcd* (*5*). *Nna1* was also expressed in mature and developing sperm (Fig. 5J), consistent with the defective spermatogenesis in *pcd* (*5*, *12*).

Although no abnormalities have been described within the hippocampus or cerebral cortex of *pcd* mice (*20*), neurons in these structures robustly express *Nna1* (data not shown) (Fig. 5L) [see also (*15*)]. Thus, absolute levels of *Nna1* expression do not predict neuronal vulnerability. This may result from genetic redundancy because *Caenorhabditis elegans* harbors two *Nna1*-related genes (*15*), and human and mouse genomes contain genes encoding proteins with similar structures to Nna1.

The identification of *Nna1* as the gene mutated in *pcd* mice provides an unexpected link between neuronal degeneration and regeneration. Because axotomy triggers induction of *Nna1* in spinal motor neurons (*15*), *pcd* mice may provide a valuable paradigm to investigate molecular mechanisms of axonal regeneration. Indeed, some of the cytological features of degenerating thalamic neurons in *pcd* resemble those of axotomized neurons (*6*). It remains to be elucidated whether mutation or altered expression of NNA1 or NNA1-related genes underlies or modifies other hereditary or sporadic neurodegenerative diseases. Lastly, because Nna1 harbors a zinc carboxypeptidase domain that is essential in AEBP1 (*21*), it may be a target for modifying neuronal survival and/or male fertility.

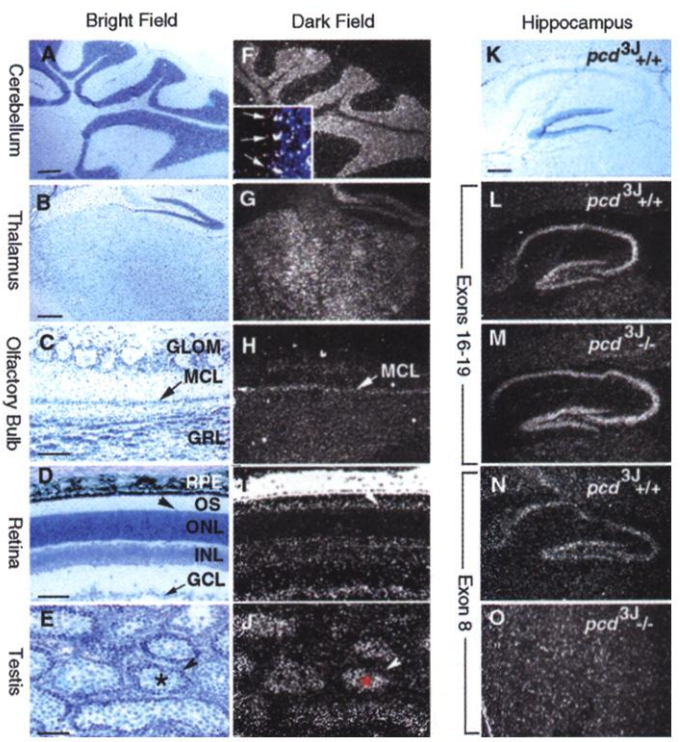

Fig. 5. In situ hybridization of *Nna1* in brain, eye, and testis. (**A**), (**B**), (**C**), (**D**), (**E**), and (**K**) show bright-field microscopy of 1-month-old wild-type mouse. (**F**), (**G**), (**H**), (**I**), and (**J**) show corresponding dark-field microscropy using an antisense probe derived from exons 16-19. (A) and (F), cerebellum; (B) and (G), thalamus; (C) and (H), olfactory bulb; (D) and (I), retina; (E) and (J), testis; (**L**) and (**M**), hippocampus of *pcd*^{3J}+/+ (L) and *pcd*^{3J}−/− (M) hybridized with probe derived from exons 16 to 19. Hippocampus of *pcd*^{3J}+/+ (**N**) and *pcd*^{3J}−/− (**O**) hybridized with an antisense probe derived from exon 8. Inset in (F), higher magnification showing Purkinje cells (arrows) that are strongly positive. In (B) and (G), thalamic neurons are *Nna1*-positive. In (C) and (H), abbreviations are as follows: GLOM, glomerular layer; MCL, mitral cell layer (arrows); GRL, granule cell layer. Mitral cells are *Nna1*-positive. In (D) and (I): RPE, retinal pigment epithelium; OS, outer segment; ONL, outer nuclear layer; INL, inner nuclear layer; GCL, retinal ganglion layer (arrow). The inner segments (arrowheads) of photoreceptors are *Nna1*-positive. In (E) and (J), the region containing Sertoli cells and spermatogonia (arrowheads) are *Nna1*-negative, whereas the region containing more mature components of spermatogenesis and sperm (asterisks) are *Nna1*-positive. In (L) and (M), the exon 16 to 19 probe exhibits similar hybridization patterns in hippocampus of *pcd*^{3J}+/+ and *pcd*^{3J}−/−. In (N) and (O), the exon 8 probe does not hybridize to the *pcd*^{3J}−/− hippocampus. Scale bar for (A), (B), (F), (G), and (K) through (O), 75 μm; bar for (C) and (H), 40 μm; bar for (D), (E), (I), and (J), 20 μm.

References and Notes

1. R. L. Sidman, M. C. Green, S. H. Appel, *Catalog of the Neurological Mutants of the Mouse* (Harvard University Press, Cambridge, MA, 1965).
2. M. E. Hatten, J. Alder, K. Zimmerman, N. Heintz, *Curr. Opin. Neurobiol.* **7**, 40 (1997).
3. N. Heintz, H. Y. Zoghbi, *Annu. Rev. Physiol.* **62**, 779 (2000).
4. S. C. Landis, R. J. Mullen, *J. Comp. Neurol.* **177**, 125 (1978).
5. R. J. Mullen, E. M. Eicher, R. L. Sidman, *Proc. Natl. Acad. Sci. U.S.A.* **73**, 208 (1976).
6. S. O'Gorman, *J. Comp. Neurol.* **234**, 298 (1985).
7. ———, R. L. Sidman, *J. Comp. Neurol.* **234**, 277 (1985).
8. C. A. Greer, G. M. Shepherd, *Brain Res.* **235**, 156 (1982).
9. M. M. LaVail, J. C. Blanks, R. J. Mullen, *J. Comp. Neurol.* **212**, 217 (1982).
10. J. C. Blanks, R. J. Mullen, M. M. LaVail, *J. Comp. Neurol.* **212**, 231 (1982).
11. R. J. Mullen, M. LaVail, *Nature* **258**, 528 (1975).
12. M. A. Handel, M. Dawson, *Gamete Res.* **4**, 185 (1981).
13. A. Servadio, A. McCall, H. Zoghbi, E. M. Eicher, *Genomics* **29**, 812 (1995).
14. D. B. Campbell, E. J. Hess, *Brain Res. Mol. Brain Res.* **37**, 79 (1996).
15. A. Harris *et al.*, *Mol. Cell. Neurosci.* **16**, 578 (2000).
16. A. Fernandez-Gonzalez, I. Perez-Otano, J. I. Morgan, *Eur. J. Neurosci.* **12**, 1573 (2000).
17. B. A. Hamilton *et al.*, *Neuron* **18**, 711 (1997).
18. J. A. Blake, J. T. Eppig, J. E. Richardson, C. J. Bult, J. A. Kadin, *Nucleic Acids Res.* **29**, 91 (2001).
19. R. J. Mullen, *Nature* **270**, 245 (1977).
20. C. R. Goodlett, K. M. Hamre, J. R. West, *Behav. Brain Res.* **47**, 129 (1992).
21. G. P. He, A. Muise, A. W. Li, H. S. Ro, *Nature* **378**, 92 (1995).
22. For long-distance PCR, protocols of Takara *Ex Taq* polymerase (PanVera Corporation, Madison, WI) were followed using genomic DNA as templates.

23. We thank B. Sopher, R. Martinez, P. Bailey, and R. Bronson for technical expertise; E. Eicher for DNA samples and mapping of the CAST/Ei x *pcd*^{1J} cross; M. Davisson and K. Johnson for support of initial characterization of *pcd*^{3J}; N. Heintz and H. Soares for advice; and T. Curran for critical comments. Supported in part by NIH Cancer Center Support CORE grant CA21765, the American Lebanese Syrian Associated Charities (ALSAC), the March of Dimes Birth Defects Foundation (#5-FY98-0725 to J.Z.), the Christopher Reeve Paralysis Foundation (MBC1-0001 to J.I.M.), the A-T Children's Project (to R.L.S.), and NIH grants (EY 12950 and DC 04761 to J.Z., NS 40361 and ES 10772 (to J.I.M.), CA 23944 (to J.C.H.), and RR 01183 (to B.S.H.)).

11 December 2001; accepted 29 January 2002